

# Non-Linear behavior of Raman Linewidth of 1-3 Layer WSe<sub>2</sub>

E. Easy,<sup>1,a)</sup> J. Hernandez,<sup>1,a)</sup> T. Chou,<sup>1</sup> X. Zhang<sup>1,b)</sup>

<sup>1</sup>*Mechanical Engineering Department, Stevens Institute of Technology, Hoboken, New Jersey, 07030, USA*

In recent years, Raman spectroscopy of two-dimensional (2D) materials has been conducted. However, only a small portion of those studies note the full width half maximum (FWHM) of these 2D materials. FWHM is an indicator of phonon dispersions in 2D materials. In addition, it is a critical parameter that can denote the quality of the given 2D material, which is directly related to its engineering performance for manufactured devices. In this study, we analyze the effect that temperature has on the FWHM of the  $E_{2g}^1$  mode for WSe<sub>2</sub>. We also analyze this temperature dependent trend for WSe<sub>2</sub> with different thicknesses: monolayer (1L), bilayer (2L), and triple-layer (3L). The results show a different trend associated with each thickness on temperature dependence analysis for WSe<sub>2</sub>. The 1L WSe<sub>2</sub> shows a parabolic trend with increasing temperature. Meanwhile, the 2L shows a steady linear trend with increasing temperature. On the other hand, FWHM for 3L WSe<sub>2</sub> can be fitted by a simplified Klemens model, which explains its non-linear behavior.

## I. INTRODUCTION

In recent years, abundant studies have been done on the extraordinary properties of graphene and transition-metal dichalcogenides (TMDs) <sup>1,2</sup>.

---

<sup>a</sup>Easy E. and Hernandez J. contributed equally to this work.

<sup>b</sup>Zhang X. is the correspondence Author who should be addressed. Electronic mail: [xzhang4@stevens.edu](mailto:xzhang4@stevens.edu)

One of the more exciting features which scientists have focused on is the electronic structure of 2D TMDs materials compared to their bulk phases<sup>3,4,5</sup>. The direct bandgap of 1L TMDs and 2D materials enhances the optoelectronic application possibilities such as solar cells and thermoelectricity<sup>6,7,8,9,10,11</sup>. WSe<sub>2</sub> is a promising candidate due to its low thermal conductivity at room temperature<sup>12,13,14,15,16,17</sup> and the high Seebeck coefficient of about 680  $\mu\text{V/K}$ , which results in the high figure of merits<sup>18,19</sup>.

Raman spectroscopy is the precise and clean method to study the thermal properties of 2D materials. The Raman spectrum for 2D materials, e.g., MoS<sub>2</sub>, and WSe<sub>2</sub> are layer-number dependent<sup>10,20,21</sup>. WSe<sub>2</sub> has a layer-dependent trend and, as a result, has attracted a lot of research on electron transport in WSe<sub>2</sub><sup>20,22,23,24</sup>. However, phonon transport has received less attention, and few experimental data investigates phonon scattering properties in few-layer WSe<sub>2</sub><sup>25,26,27,28</sup>. As the laser shines on the surface, it causes thermal expansion and change in the lattice constant, leading to phonon frequency shift<sup>29</sup>. Furthermore, analyzing the Raman spectra allows for the study of phonon-phonon interactions<sup>30,31</sup>. Phonon scattering properties can be further investigated by their decay time which can be experimentally studied by their FWHM or linewidth of the Raman spectrum<sup>32,33</sup>.

The study of temperature dependent phonon properties revealed acoustic and optical phonon scattering effects on carrier mobility<sup>34</sup>. FWHM of different numbers of layers for WSe<sub>2</sub> promotes understanding about vibrational modes and anharmonic phonon-phonon interaction for different thicknesses<sup>33,35</sup>.

Between the WSe<sub>2</sub> active Raman modes,  $A_{1g}$  mode has a weak Raman intensity, preventing us from analyzing the data. Although, the  $E_{2g}^1$  mode high intensity provides us with helpful information about the phonon scattering and lifetime<sup>33,35</sup>.

Z. Li, Y. Wang, et al.<sup>33</sup> reported that the Lorentzian function is the best fit for 1-5 layers of WSe<sub>2</sub> Raman linewidth, and it shows the increasing linear trend with increasing temperature. However, L. P. McDonnell, J. S. Viner, et al.<sup>36</sup> reported the non-linear FWHM trend for 1L WSe<sub>2</sub> and noted the excitonic dispersion relations is a possible explanation. Still, the theoretical principle and science behind this phenomenon have not been discussed.

Experimental assessment of the in-plane thermal conductivity of WSe<sub>2</sub> is so essential to understand the phonon scattering behavior and science behind this phenomenon of this 2D material. Hence in this work, we focused on the Raman spectra of 1-3 layers of WSe<sub>2</sub>. We studied the FWHM of each spectrum to bridge the theoretical prediction and experimental data gap; moreover, the explanation behind this has been comprehensively discussed.

## II. RESULT AND DISCUSSIONS

WSe<sub>2</sub>, like graphite, has a lamellar structure; van der Waals (vdW) interaction holds the layers stacked, and 2D layers can be achieved by exfoliation. The molecular structure consists of tungsten atoms sandwiched between selenium with trigonal geometry. Figure (1) shows both the optical microscopy imaging and atomic force microscopy (AFM) analysis of the 1, 2, and 3 layers of WSe<sub>2</sub> flakes<sup>37</sup>. Figure (2) provides the Raman spectrum of WSe<sub>2</sub>, which proves the existence of 1-3 layers<sup>29</sup>.

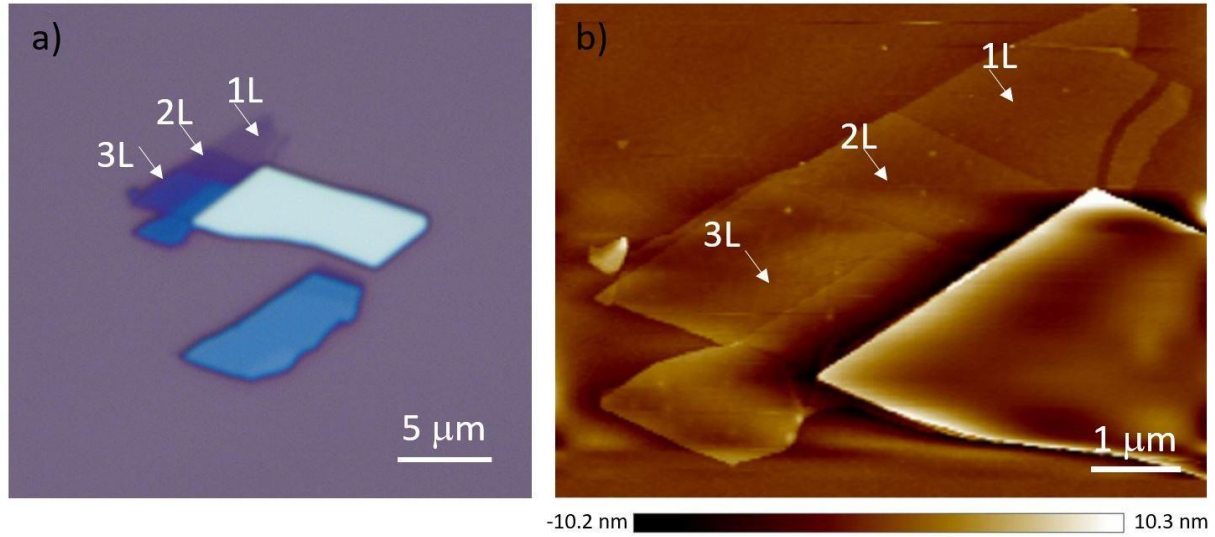


FIG. 1. a) Optical image of 1-2 and 3 Layers of WSe<sub>2</sub>. b) AFM image of the same flakes to identify the number of layers<sup>37</sup>.

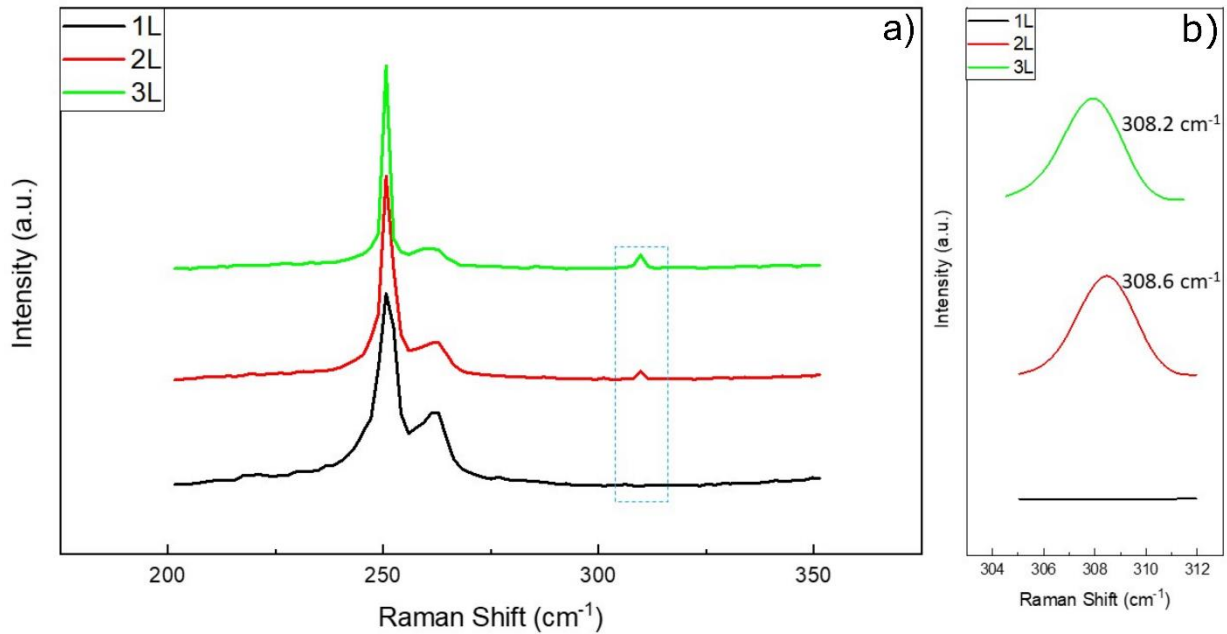


FIG. 2. (a) The Entire Raman spectrum for 1-2-and 3 layers of WSe<sub>2</sub>. The 1L is shown by the black line, 2L by red line, and 3L layers by green lines. A part of the Raman spectra (a) has been magnified, indicated by the blue dashed rectangle (b). The numbers next to each peak in (b) denote the center peak positions<sup>29</sup>.

To achieve quantitative analysis, we need to use the semi-quantitative model. Thermal expansion and pure thermal effect are the two effects we are taking into account<sup>33</sup>.

$$\omega(T) = \omega_0 + \Delta\omega_E(T) + \Delta\omega_A(T) \quad (1)$$

Where  $\Delta\omega_E(T)$  represent the Raman shift caused by thermal expansion and  $\Delta\omega_A(T)$  is the Raman shift for temperature effect.  $\omega_0$  is the frequency at zero Kelvin. Its value is achieved by fitting the linear curve.

To describe the thermal expansion, we are using the Grüneisen constant model<sup>33</sup>.

$$\Delta\omega_E = \omega_0 \exp\left(-n\gamma \int_0^T \alpha dT\right) - \omega_0 \quad (2)$$

Where  $\alpha$  is the thermal expansion coefficient, n describe the degeneracy of  $E_{2g}^1$  mode equal to 2, and  $\gamma$  is the Grüneisen parameter with the following equation:

$$\gamma\alpha = a + bT + cT^2 \quad (3)$$

Where a, b, and c can be obtained by fitting to non-linear temperature dependent Raman spectrum. By substituting equation (3) in equation (2), we will have

$$\Delta\omega_E(T) = \omega_0 \exp\left(-2aT - bT^2 - \frac{2}{3}cT^3\right) - \omega_0 \quad (4)$$

The temperature effect can be considered as an anharmonic effect of phonon scattering. Due to non-harmonic interactions, the decay of optical phonons into two phonons or three phonons occurs. These interactions are considered as three-phonon and four-phonon scattering processes, respectively<sup>33</sup>. As previously stated, the semi-quantitative model can mathematically explain the temperature effect.

$$\Delta\omega_A(T) = d \left[1 + \frac{2}{\exp(\hbar\omega/2KT)-1}\right] + f \left[1 + \frac{3}{\exp(\hbar\omega/3KT)-1} + \frac{3}{(\exp(\hbar\omega/3KT)-1)^2}\right] \quad (5)$$

Where  $\hbar\omega$  is the Raman mode vibrational energy, T is the temperature (Kelvin), K is the Boltzman constant, d and f are the contributions of phonon scattering frequency shift<sup>33</sup>.

The FWHM of  $E_{2g}^1$  Raman mode shows the broadening of the phonon modes. Harmonic modes interact with each other causing non-harmonic forces, and as a result, the optical phonon lifetime decreases, and broadening happens<sup>24</sup>.

$$\Gamma(T) = \Gamma_0 + C \left[ 1 + \frac{1}{\exp(\hbar\omega_1/KT)} + \frac{1}{\exp(\hbar\omega_2/KT)} \right] \quad (6)$$

Where  $\Gamma_0$  describes broadening due to temperature-independent defects, and C represents the broadening due to phonon decay<sup>33</sup>. The exponential quantities are Bose-Einstein distribution at frequencies  $\omega_1$  and  $\omega_2$  representing the different phonon scattering modes.

Furthermore, in some materials, the temperature dependence of the FWHM of  $E_{2g}^1$  Raman mode could be due to four-phonon scattering processes. Rather than a semi-quantitative model, a simplified Klemens model is used. The simple Klemens assumes that the decay of one optical phonon into three acoustic phonons is symmetrical, producing three phonons of the same wavenumber<sup>38</sup>.

$$\Gamma(T) = A \left[ 1 + \frac{2}{\exp(\hbar\omega_0/2KT)-1} \right] + B \left[ 1 + \frac{3}{\exp(\hbar\omega_0/3KT)-1} + \frac{3}{(\exp(\hbar\omega_0/3KT)-1)^2} \right] \quad (7)$$

Figures (3-5) shows the linewidth temperature dependence for 1-layer (1L), 2-layer (2L), and 3-layer (3L) WSe<sub>2</sub> for the  $E_{2g}^1$  peak FWHM showing both the actual experimental data and the derived equations.

The quantitative expression for the 1L WSe<sub>2</sub>  $E_{2g}^1$  peak linewidth temperature dependence, described by the black curve in figure (3), is the combination of both lattice thermal expansion and anharmonic phonon scattering processes. The modified Grüneisen parameter shown in equation (4) describes the Lorentzian fit FWHM as a function of thermal expansion. In the interim, equation (5) describes the FWHM as a function of three-phonon decay processes using a semi-quantitative

model. Previous work<sup>33</sup> represents the Lorentzian fit for FWHM only depends on the temperature effect and results in a linear fit. However, such a linear fit is not sufficient to explain 1L WSe<sub>2</sub> as it is shown to have a non-linear temperature dependence. Figure (3) shows that both the thermal expansion and phonon scattering effects result in a more accurate non-linear fit. The well-fitted model offers a similar non-linear decrease up to 300K followed by a non-linear increase after 300K.

Initially, the data for 1L WSe<sub>2</sub> is shown to have a non-linear decrease with an increase of temperature up to approximately 300K. We assume that there are a few phenomena that may be able to explain this initial decreasing trend in 1L WSe<sub>2</sub>. First of all, the decreasing trend could be explained in terms of the degenerative nature of 1L WSe<sub>2</sub>. As confirmed by other groups,<sup>31</sup> 1L WSe<sub>2</sub> is virtually degenerate; meanwhile, degeneracy disappears for 2L or more. Alternatively, there might be contributions from inactive Raman phonon modes that cause this trend. It is known that WSe<sub>2</sub> has multiphonon bands consisting of these inactive Raman modes located either at the Brillouin zone center or zone edge<sup>29</sup>. Furthermore, some multiphonon bands are only present in multilayer WSe<sub>2</sub> and absent in 1L, suggesting that there are contributions from low frequency modes such as  $E_{2g}^2$ . With an increase in temperature, however, these contributions may lessen, making  $E_{2g}^1$  the dominant mode and causing that initial decrease as seen in figure (3). Another phenomenon that may explain the initial decline is the possibility of background photoluminescence (PL). 1L WSe<sub>2</sub> can cause second harmonic generation (SHG), meaning that a small portion of the incident Raman laser is scattered at a different wavelength than the originating laser. These backscattered photons can be absorbed along with the laser photons; this two-photon absorption induces background PL. We assume that the generation of the background PL is responsible for the thermal lattice expansion present in the 1L WSe<sub>2</sub><sup>39</sup>.

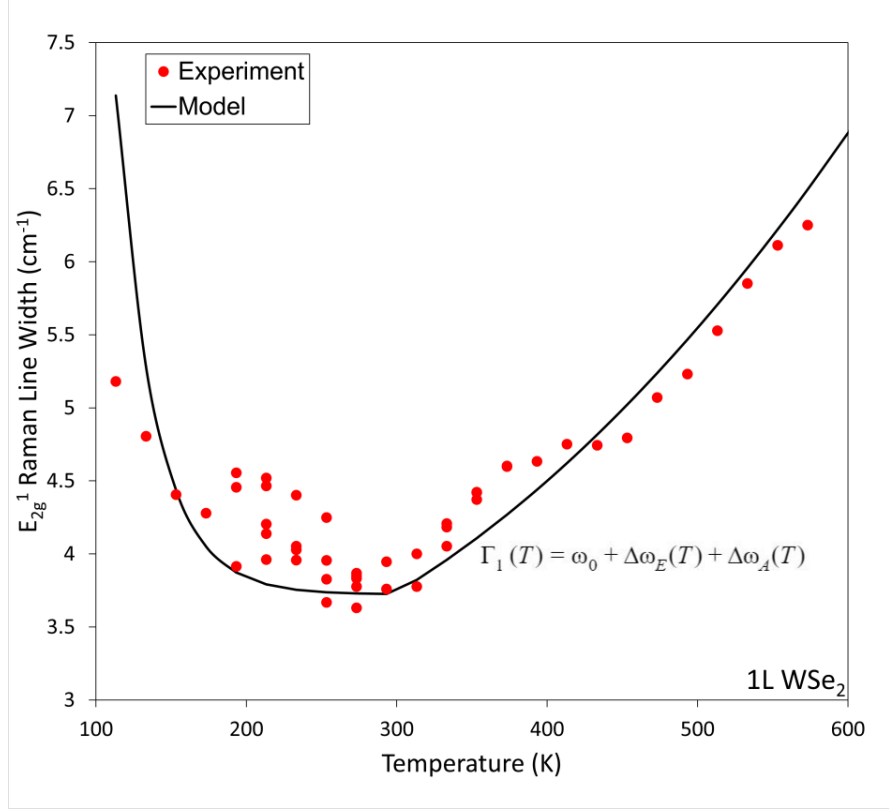


FIG. 3. FWHM of 1L WSe<sub>2</sub>. Red dots are the experimental result, and the black line is the theoretical data fitting it. The parabolic trend combines the Grüneisen constant model for thermal expansion and the semi-quantitative model to describe the temperature effect.

Interestingly enough, the data for 2L WSe<sub>2</sub>  $E_{2g}^1$  peak linewidth temperature dependence, shown in figure (4), can be fitted linearly. This linear fit is described in equation (6), where the inverse exponential terms represent the Bose-Einstein distribution. The experimental data can be fitted to this modified Bose-Einstein distribution, where  $C$ ,  $\Gamma_0$ ,  $\omega_1$ , and  $\omega_2$  are fitting parameters. Qualitatively this expression describes the temperature dependent linewidth as a function of both three-phonon scattering processes and crystalline defects. Here, the interaction of two different modes of three-phonon scattering is shown by the two different Bose-Einstein distribution quantities, demonstrates a similar linearly increasing trend with an increase in temperature.



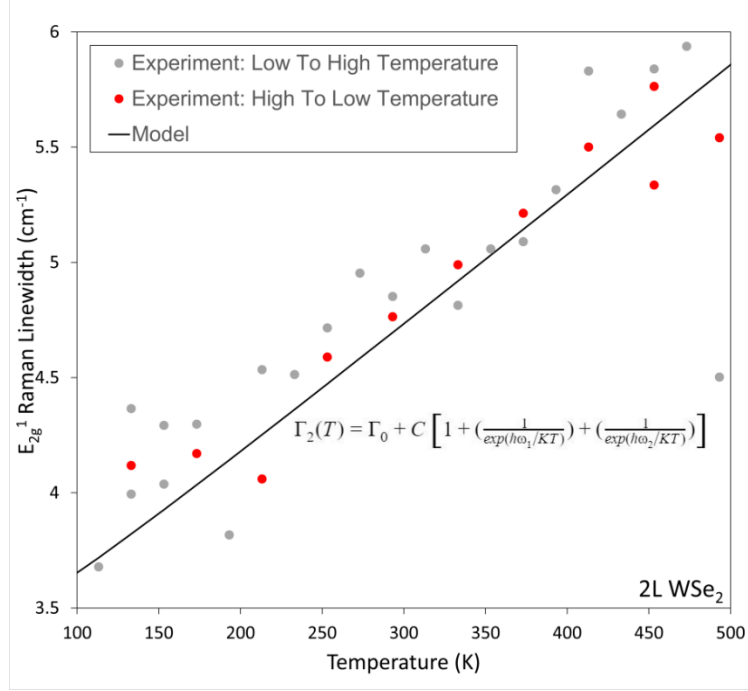


FIG. 4. FWHM of bilayer WSe<sub>2</sub>. Red dots are the experimental result, and the black line is the theoretical data fitting it. Modified Bose-Einstein distribution can be used to explain the increasing trend with increasing temperature.

The  $E_{2g}^1$  peak FWHM temperature dependence for 3L WSe<sub>2</sub>, shown in figure (5), offers a dissimilar trend to both 1L and 2L. This non-linear fit can be best described by equation (7) based on a simplified Klemens model. For 3L WSe<sub>2</sub>, the dominant process for FWHM temperature dependence is the symmetric four-phonon scattering process. Despite the simplifications made, the simplified Klemens model can quantitatively describe the temperature dependent FWHM in the  $E_{2g}^1$  peak. After proper data fitting using the adjustable parameters A and B, both the data and simplified Klemens model show a non-linear increase with increasing temperatures.

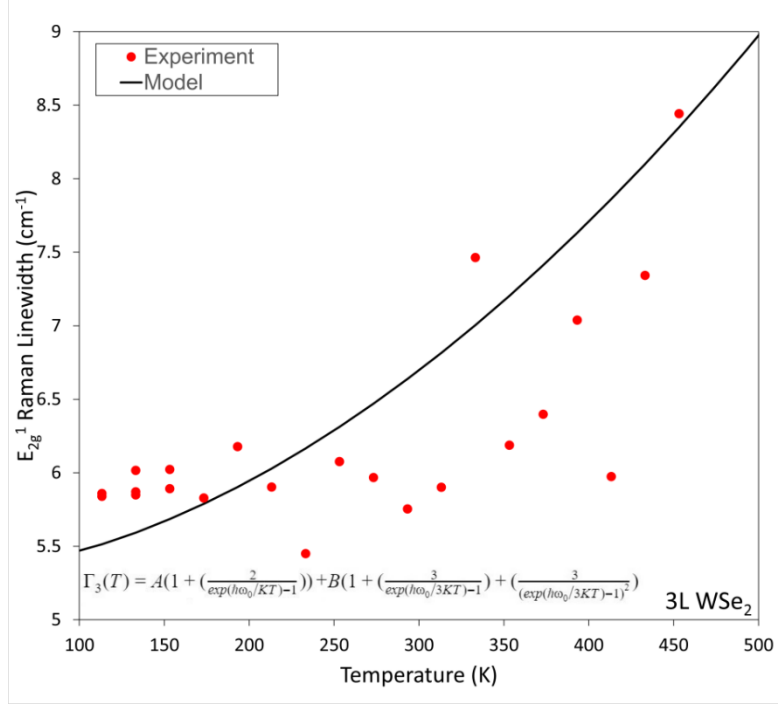


FIG. 5. FWHM of Three-layer WSe<sub>2</sub>. Red dots are the experimental result, and the black line is the theoretical data fitting it. Simplified Klemens model can fit the non-linear trend with increasing temperature.

As shown in figures (3, 4, and 5), different amounts of layers in WSe<sub>2</sub> have other trends concerning increasing temperatures for the temperature dependent FWHM of  $E_{2g}^1$  peaks. Multiple mechanisms are the main reason behind these various trends for temperature dependence linewidths. These different mechanisms may originate from interlayer interactions at different layer amounts, such as variations in vdW interactions and the weak phonon interactions between layers. The latter causes decreased thermal transport in 2D materials and reducing the phonon lifetime<sup>39</sup>.

### III. CONCLUSION

To summarize, we have performed an experimental investigation on the FWHM of WSe<sub>2</sub> at both varying layer thickness and temperature conditions. Measurements for the 1L, 2L, and 3L WSe<sub>2</sub> Lorentzian fit FWHM at a temperature range of 100K to 500K for  $E_{2g}^1$  mode was obtained. Results show that all triple-layer thicknesses have different trends with respect to an increasing

temperature. The WSe<sub>2</sub> FWHM temperature dependence has a different trend based on the number of layers. Interestingly, the 1L WSe<sub>2</sub> shows an initial decrease for the temperature up to 300K, followed by a non-linear increase. The parabolic trend of 1L WSe<sub>2</sub> is a combination of thermal expansion and temperature effect. The temperature dependent FWHM can be fitted to modified Grüneisen parameter and semi-quantitative model. The linearity of 2L WSe<sub>2</sub> primarily originates from the three-phonon scattering process that the Lorentzian model can explain. However, the non-linear nature for 3L WSe<sub>2</sub> is due to a symmetrical four-phonon decaying process. The FWHM can be fitted using a simplified Klemens model to explain its non-linear trend. Understanding that both these processes are critical contributors to the FWHM of 1L WSe<sub>2</sub> yields a more accurate non-linear fit for our data. This work will shed light on discovering the fundamental mechanisms of phonon dispersions in 2D materials.

#### **IV. METHOD**

Bulk crystals of WSe<sub>2</sub> (2Dsemiconductors) were mechanically exfoliated onto Si/SiO<sub>2</sub>. 1 to 3 layers of WSe<sub>2</sub> are identified under an optical microscope (Nikon Eclipse). The layer thickness was then measured by Atomic force microscopy (AFM) (Bruker Dimension), and Raman spectroscopy analysis has been used as a confirmation (see figure 1). Raman spectrum was obtained through a 514 nm laser (Renishaw Inc.). Theoretical calculations for linewidth were performed through Matlab to fit the Lorentzian, semi-quantitative, and Klemens model to our experimental result.

#### **ACKNOWLEDGEMENTS**

This work was supported by Stevens Institute of Technology's startup funding, Stevens Institute of Technology's Bridging Award, Brookhaven National Laboratory Center for Functional Nanomaterials, and Columbia Nano Initiative.

### Data Availability Statement

The data that supports the findings of this study are available within the article.

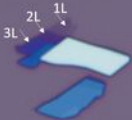
### REFERENCES

- <sup>1</sup>Li, Z., Xu, B., Liang, D., Pan, A., “Polarization-Dependent Optical Properties and Optoelectronic Devices of 2D Materials”, *Research*, 5464258-35 (2020)
- <sup>2</sup>Ye, F., Liu, Q., Xu, B., X.-L. Feng, P., Zhang, X., “Very High Interfacial Thermal Conductance in Fully hBN-Encapsulated MoS<sub>2</sub> van der Waals Heterostructure”, 2102.05239 (2021)
- <sup>3</sup>Tonndorf, P., Schmidt, R., Böttger, P., Zhang, X., Bärner, J., Liebig, A., Albrecht, M., Kloc, C., Gordan, O., Dietrich, R., et al., “Photoluminescence Emission and Raman Response of Monolayer MoS<sub>2</sub>, MoSe<sub>2</sub>, and WSe<sub>2</sub>.” *Opt. Express* 21, 4908–4916 (2013)
- <sup>4</sup>Zibouche, N., Heine, T., “Influence of Quantum Confinement on the Electronic Structure of the Transition Metal Sulfide TS<sub>2</sub>”, *Phys. Rev. B*, 83, 245213 (2011)
- <sup>5</sup>Ghorannevis, Z., Chu, L., Toh, M., Kloc, C., Tan, P.-H., Eda, G., “Evolution of Electronic Structure in Atomically Thin Sheets of WS<sub>2</sub> and WSe<sub>2</sub>.” *ACS Nano* 7, 791–797 (2013)
- <sup>6</sup>Mak, K. F., Lee, C., Hone, J., Shan, J., Heinz, T. F., “Atomically Thin MoS<sub>2</sub>: A New Direct-Gap Semiconductor”, *Phys. Rev. Lett.* 105, 136805 (2010)
- <sup>7</sup>Dariani R. S., Easy E., “Fabrication of TiO<sub>2</sub> nanostructures on TiO<sub>2</sub>/Au/quartz device for solar cell applications”, *Optik* 126, 3407–3410 (2015)
- <sup>8</sup>Novoselov K. S., Geim A. K., Morozov S. V., Jiang D., Dubonos S. C., Grigorieva I. V., Firsov A. A., “Electric Field Effect in Atomically Thin Carbon Films”, *Science* 306, 666-669 (2004)
- <sup>9</sup>Geim A. K., Novoselov K. S., “The Rise of graphene”, *Nature Materials* 6, 183-191 (2007)
- <sup>10</sup>Li, Y., Chernikov, A., Zhang, X., Rigosi, A. H., H. Zande, A. M., Chenet, D. A., Shih, E., Hone, J., Heinz, T. F., “Measurement of the optical dielectric function of monolayer transition-metal dichalcogenides: MoS<sub>2</sub>, MoSe<sub>2</sub>, WS<sub>2</sub>, and WSe<sub>2</sub>”, *Phys. Rev. B* 90, 205422 (2014)
- <sup>11</sup>Cui, X., Lee, G. H., Kim, Y. D., Arefe, G., Huang, P. Y., Lee, C. H., Chenet, D. A., Zhang, X., Wang, L., Ye, F., Pizzocchero, F., Jessen, B. S., Watanabe, K., Taniguchi, T., Muller, D. A., Low, T., Kim, P., Hone, J., “Multi-terminal transport measurements of MoS<sub>2</sub> using a van der Waals heterostructure device platform”, *Nat. Nanotechnol.* 534–540 (2015)
- <sup>12</sup>Wang J., Xie F., Cao X.H., An S.-C., Zhou W.-X., Tang L.-M., Chen K.-Q., “Excellent Thermoelectric Properties in monolayer WSe<sub>2</sub> Nanoribbons due to Ultralow Phonon Thermal Conductivity”, *Scientific Reports* 7, 41418 (2017)
- <sup>13</sup>Zhou W.-X., Chen K.-Q., “First-Principles Determination of Ultralow Thermal Conductivity of monolayer WSe<sub>2</sub>”, *Scientific Reports* 5, 15070 (2015)

- <sup>14</sup>Norouzzadeh P., Singh D. J., “Thermal conductivity of single-layer WSe<sub>2</sub> by a Stillinger–Weber potential”, *Nanotechnology* 28, 075708 (2017)
- <sup>15</sup>Fang, H., Chuang, S., Chang, T. C., Takei, K., Takahashi, T., Javey, A., “High-Performance Single Layered WSe<sub>2</sub> p-FETs with Chemically Doped Contacts”, *Nano Lett.* 3788– 3792 92 (2012)
- <sup>16</sup>Cai, Q. R., Scullion, D., Gan, W., Falin, A., Zhang, S. Y., Watanabe, K., Taniguchi, T., Chen, Y., Santos, E. J. G., Li, L. H., “High thermal conductivity of high-quality monolayer boron nitride and its thermal expansion”, *Sci. Adv.*, eaav0129 (2019)
- <sup>17</sup>Bae, J. J., Jeong, H. Y., Han, G. H., Kim, J., Kim, H., Kim, M. S., Moon, B. H., Lim, S. C., Lee, Y. H., “Thickness-dependent in-plane thermal conductivity of suspended MoS<sub>2</sub> grown by chemical vapor deposition”, *Nanoscale* 2541– 2547 (2017)
- <sup>18</sup>Easy E., Gao Y., Wang Y., Yan D., Goushehgir S. M., Yang E.H., Xu B., Zhang X., “Experimental and Computational Investigation of Layer-Dependent Thermal Conductivities and Interfacial Thermal Conductance of One- to Three-Layer WSe<sub>2</sub>”, *ACS Applied Materials & Interfaces* 13 (11), 13063-13071 (2021)
- <sup>19</sup>Kumar, S., Schwingenschlogl, U., “Thermoelectric Response of Bulk and Monolayer MoSe<sub>2</sub> and WSe<sub>2</sub>”, *Chem. Mater.* 27, 1278– 1284 (2015)
- <sup>20</sup> Sahin, H., Tongay, S., Horzum, S., Fan, W., Zhou, J., Li, J., Wu, J., Peeters, F. M., “Anomalous Raman spectra and thickness-dependent electronic properties of WSe<sub>2</sub>”, *Phys. Rev. B* 87, 165409 (2013)
- <sup>21</sup>Najmaei, S., Ajayan, P. M., Lou, J., “Quantitative analysis of the temperature dependency in Raman active vibrational modes of molybdenum disulfide atomic layers”, *Nanoscale* 5, 9758– 9763 (2013)
- <sup>22</sup>Yuan X. W. H., Lian B., Zhang H., Fang X., Shen B., Xu G., Xu, Y., Cui, Y.,, “Generation and electric control of spin–valley-coupled circular photogalvanic current in WSe<sub>2</sub>”, *Nature Nanotechnology* 9, 851-857 (2014)
- <sup>23</sup>Wang Y., Gao Y., Easy E., Yang E. -H., Xu B., Zhang X., “Thermal Conductivities and Interfacial Thermal Conductance of 2D WSe<sub>2</sub>”, 2020 IEEE 15th International Conference on Nano/Micro Engineered and Molecular System (NEMS), 575-579 (2020)
- <sup>24</sup>Gasanly, N. M., Aydınli, A., Özkan, H., Kocabaş, C., “Temperature Dependent Raman scattering spectra of ε-GaSe layered crystal”, *Materials Research Bulletin* 37, 169–176 (2002)
- <sup>25</sup>Seyler, K., Schaibley, J., Gong, P., Rivera P., Jones A. M., Wu S., Yan J., Mandrus D. G., Yao W., Xu X., “Electrical control of second-harmonic generation in a WSe<sub>2</sub> monolayer transistor”, *Nature Nanotech* 10, 407–411 (2015)
- <sup>26</sup>Huang J., Hoang T., Mikkelsen M. H., “Probing the origin of excitonic states in monolayer WSe<sub>2</sub>”, *Scientific Reports* 6, 22414 (2016)

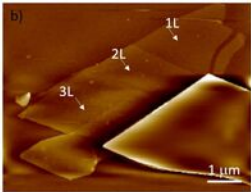
- <sup>27</sup>Jiang P., Qian X., Gu X., Yang R., “Probing Anisotropic Thermal Conductivity of Transition Metal Dichalcogenides  $\text{MX}_2$  ( $\text{M} = \text{Mo W}$  and  $\text{X} = \text{S Se}$ ) using Time-Domain Thermoreflectance”, *Advanced Materials* 29, 1701068 (2017)
- <sup>28</sup>Late, D. J., Shirodkar, S. N., Waghmare, U. V., Dravid, V. P., Rao, C. N. R., “Thermal expansion, anharmonicity and temperature-dependent Raman spectra of single- and few-layer  $\text{MoSe}_2$  and  $\text{WSe}_2$ ”, *ChemPhysChem* 15, 1592–1598 (2014)
- <sup>29</sup>Zhao W., Ghorannevis Z., Amara K. K., Pang J. R., Toh M., Zhang X., Kloc C., Tane P. H., Eda G., “Lattice dynamics in mono- and few-layer sheets of  $\text{WS}_2$  and  $\text{WSe}_2$ ”, *Nanoscale* 5, 9677-9683 (2013)
- <sup>30</sup>Kaasbjerg, K., Thygesen, K. S., Jacobsen, K. W., “Phonon-limited mobility in n-type single-layer  $\text{MoS}_2$  from first principles”, *Phys. Rev. B* 85, 115317 (2012)
- <sup>31</sup>Kash J.A., Tsang J.C., Light scattering and other secondary emission studies of dynamic processes in semiconductors. In: Cardona M., Güntherodt G. (eds) *Light Scattering in Solids VI*, Applied Physics, Springer, Berlin, Heidelberg. 3540536140-24-423 (1991)
- <sup>32</sup>Debernardi, A. and Ulrich, C. and Syassen, K. and Cardona, M., “Raman linewidths of optical phonons in 3C–SiC under pressure: First-principles calculations and experimental results”, *Phys. Rev. B* 59, 6774 (1999)
- <sup>33</sup>Li Z., Wang Y., Jiang J., Liang Y., Zhong B., Zhang H., Yu K., Kan G., Zou M., “Temperature-dependent Raman spectroscopy studies of 1–5-layer  $\text{WSe}_2$ ”, *Nano Research* 13, 591–595 (2020)
- <sup>34</sup>Park K. H., Mohamed M., Aksamija Z., Ravaioli U., “Phonon scattering due to van der Waals forces in the lattice thermal conductivity of  $\text{Bi}_2\text{Te}_3$  thin films”, *Journal of Applied Physics* 117, 015103 (2015)
- <sup>35</sup>Mavrokefalos A., Nguyen N. T., Pettes M. T., Johnson D. C., Shi L., “In-plane thermal conductivity of disordered layered  $\text{WSe}_2$  and  $(\text{W})_x(\text{WSe}_2)_y$  superlattice films”, *Applied Physics Letters* 91, 171912 (2007)
- <sup>36</sup>McDonnell, L. P., Viner, J. J. S., Rivera, P., Xu, X., Smith, D. C., “Observation of intravalley phonon scattering of 2s excitons in  $\text{MoSe}_2$  and  $\text{WSe}_2$  monolayers”, *2D Mater.* 7 045008 (2020)
- <sup>37</sup>Berman, D., Erdemir, A., Sumant, A., “Approaches for Achieving Superlubricity in Two-Dimensional Materials”, *ACS Nano*. 12.10.1021/acsnano.7b09046-fig 11 (2018)
- <sup>38</sup>Surovtsev N. V., Kupriyanov I. N., “Temperature dependence of the Raman line width in diamond: Revisited,” *Journal of Raman Spectroscopy* 46, 171-177 (2014)
- <sup>39</sup>He K., Kumar N., Zhao L., Wang Z., Mak K. F., Zhao H., Shan J., “Tightly Bound Excitons in Monolayer  $\text{WSe}_2$ ”, *Phys. Rev. Lett.* 113, 026803 (2014)

a)



5  $\mu\text{m}$

b)



1  $\mu\text{m}$

-10.2 nm



10.3 nm

